http://dx.doi.org/10.5012/bkcs.2013.34.2.443

Synthesis of Silver Nanoplates with Fibronectin Nanofibril Template and Their SERS Applications

Li Wang,* Yujing Sun,† Yuncheng Cui, Jiku Wang, and Zhuang Li†

*College of Chemistry, Jilin Normal University, Siping 136000. *E-mail: yumo1002@yahoo.com.cn*
†State Key Laboratory of Electroanalytical Chemistry, Changchun Institute of Applied Chemistry, Chinese Academy of Sciences, Changchun 130022
Received October 4, 2012, Accepted November 14, 2012

In this work, a novel strategy is provided to prepare silver nanoplates by a fibronectin (Fn) nanofibril template. First, Fn molecules were controlled to assemble into amyloid-like nanofibrils in highly concentrated ethanol aqueous solution. The resultant nanofibrils could serve as a soft template to direct the formation of silver nanoplates. It is worth noting that the silver nanoplates are excellent surface-enhanced Raman scattering (SERS) substrate with 4-aminothiophenol (4-ATP) molecule as a test probe. This high active SERS substrate can also be used to detect drug molecule, 2-thiouracil with high sensitivity.

Key Words : Synthesis, Nanoplates, Nanofibrils, Template, SERS

Introduction

The size and shape of metal nanoparticles has been a subject of considerable interest during the last few decades owing to their unique effects on the optical, electronic, magnetic and catalytic properties of nanomaterials.[1,2] With the new generation of photoelectronic technologies and nanodevices, the nanoparticles with novel structures and shapes are in demand (*e.g.* nanowires, nanoplates and their two dimensional (2-D) and three dimensional (3-D) nanoparticle assemblages). The wide variety in shape offers opportunities to observe original chemical and physical properties and examine the mechanisms governing the growth of nanoparticles. In addition, the materials with nanoscaled sizes in one, two or three dimensions are known to have unusual physical, chemical and mechanical properties.[3] All of these advantages encourage the studies on developing new ways for the controllable preparation of well-defined 1-D, 2-D and 3-D nanostructures. Up to now, a variety of techniques are employed to prepare metal nanostructures with a certain shape and size, such as template method,[4,5] seed-mediated growth method,[6,7] electrochemical and photochemical method,[8,9] and so on. Among these approaches, template method has drawn a great deal of attention, because it is a good control over the uniformity and dimension route. Recently, a growing interest is focused on the synthesis of biomolecule-based nanostructures and materials.[10,11] Biological templates (such as DNA, proteins, bacteria, viruses, and so on) have been used to fabricate functional nanomaterials.[12] Protein fibers/nanofibrils created by the self-assembly of natural proteins are quite effective biomolecular templates for constructing nanostructures.[13,14] Relative to conventional chemical synthesis, the synthesis procedure using protein fibers/nanofibrils templates is environmentally friendly and green. The obtained products may have unexpected functional properties.

Surface-enhanced Raman scattering (SERS) is a particular and sensitive analytical tool for the detection of low-concentration analytes. Gold or silver nanoparticles as SERS active substrates have been proven to be a powerful method for research and application in the fields of analytical chemistry, biochemistry, and catalysis.[15] The SERS enhancement ability is related to the size and shape of nanoparticles. Here, we describe a novel strategy for high yield synthesis of silver nanoplates through a protein-template method. Our method provides great advantages over other methods in terms of environmentally friendly synthesis, high stability, and good biocompatibility. The nanoplates after centrifugation as SERS substrates show excellent enhancement ability, and they can be employed to detect 2-thiouracil (2-TU).

Experimental

Chemicals and Materials. Bovine plasma Fn was purchased (1 $mg \cdot mL^{-1}$) from Sigma-Aldrich Chemie GmbH (Taufkirchen, Germany). Silver nitrate ($AgNO_3$, A. R.), sodium borohydride (A. R.) and ethanol (G. R.) were supplied by Beijing chemical Reagent Co. 2-thiouracil (2-TU) was purchased from TCI (Shanghai) Development Co., Ltd. 4-aminothiophenol (4-ATP) was obtained from Alfa Aesar. All chemicals were used without further purification. The water used throughout the experiments was ultrapure water.

Synthesis of Silver Nanoplates. Preparation of Fn nanofibrils: bovine plasma Fn solution (1 $mg \cdot mL^{-1}$) was first diluted to 20 $ng \cdot \mu L^{-1}$ with water, and then 100 μL this Fn solution was mixed with ethanol at a ratio of 1:4 (v/v). After that, the mixed solution was incubated in the water-bath at 37 °C for 4 h, and Fn nanofibrils were produced.

Preparation of Silver Nanoplates: 50 μL Fn nanofibril solution was mixed with 500 μL of 10 mM $AgNO_3$ aqueous solution, and then incubated in dark for 2 h. After that, the

mixed solution was diluted with water to the concentration of Ag^+ at 4 mM, and then freshly prepared 2 mM sodium borohydride aqueous solution was added into this Ag^+ solution until the solution changed to filemot in color. The resultant colloidal solution was centrifuged at 8000 rpm for 8 min. The precipitate was collected with 1.0 cm × 1.0 cm ITO conducing glass for SERS study.

Characterization. The product morphology was characterized with a TECNAI F20 transmission electron microscope (TEM) at an accelerating voltage of 200 kV (FEI company). Tapping mode AFM images were obtained from a commercial Nanoscope IV multimode AFM (Digital Instruments, Santa Barbara, USA) at ambient temperature. SERS spectra were performed on a Renishaw 2000 model confocal microscopy Raman spectrometer with a CCD detector and a holographic notch filter (Renishaw Ltd., Gloucestershire, U.K.). Radiation of 514.5 nm from an air-cooled argon ion laser was used for the SERS excitation.

Results and Discussion

Preparation of Fn Nanofibrils. Under the inducement action of temperature, cation concentration, and pH value, proteins can self-assemble into linear-like structures through β-sheet.[5,16] In our work, highly concentrated ethanol was chosen as protein denaturant for inducing Fn molecules to assemble into nanofilbrils. Figure 1(a) shows the tapping mode AFM height image of Fn nanofibers. It can be seen that the self-assembled fibrils are long and curved. TEM image displays that these nanofibrils are thin and uniform in diameter as shown in Figure 1(b). The nanofibrils have a mean diameter of about 24 nm and a few micrometers in length. According to the report of Wei *et al*., the formation of fibrinogen nanofibrils in highly concentrated ethanol was attributed to the conformation transition of fibrinogen molecules and breakage of its secondary and tertiary structures.[5] In our case, we suggest that the introduction of ethanol into the Fn aqueous solution has the same effect to Fn molecules, and the highly concentrated ethanol causes the denaturation of Fn molecules. In this way, the Fn nanofibrils are created. Some nodes in the fibrils and branched structure can be seen in Figure 1(a) and (b). These suggest that the growth process of Fn nanofibrils is that the axial interaction increases the length of Fn nanofibrils and the lateral interaction increases the diameter.[17]

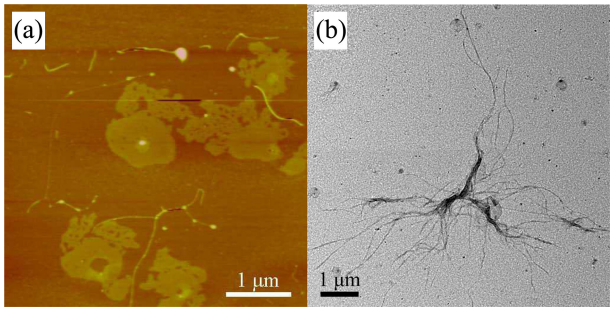

Figure 1. (a) AFM and (b) TEM image of Fn nanofibrils.

Preparation of Silver Nanoplates. The crystal structure of the silver nanoplates was investigated by TEM. The images (Figure 2(a)) reveal that the product is dominated by hexagonal and truncated triangular nanoplates. They have very smooth edges with average edge length 45 nm for hexagonal nanoplates and 44 nm for truncated triangular nanoplates as shown in the inset of Figure 2(a). Most of the nanoplates are in a state of aggregation when the sample was mounted on carbon-coated copper grids, which might be due to the evaporation action of the solvent during the drying process. Figure 2(b) gives a typical high-resolution TEM (HRTEM) image of an individual nanoplate. The clear-cut interference fringe patterns confirm the single crystallinity of this silver nanoplate. The parallel fringe space was determined to 0.248 nm that could be ascribe to the forbidden 1/3{422} reflection.[18] The inset of Figure 2(b) shows the selected area electron diffraction (SAED) pattern of the nanoplates obtained by directing the electron beam perpendicular to the planar surface of nanocrystals. The hexagonal symmetry of these pattern spots implies that these nanoplates are single crystals bounded mainly by {111} facets, and their {111} planes tend to be preferentially oriented parallel to the surface of the supporting substrate. The SAED spots was taken with the [$\bar{1}$11] zone axis oriented parallel to the electron beam. These diffraction dots could be indexed to the allowed {220}, formally forbidden 1/3{422} reflection of face-centered cubic silver. The XPS spectrum of the product shows that the binding energy of Ag $3d_{5/2}$ and Ag $3d_{3/2}$

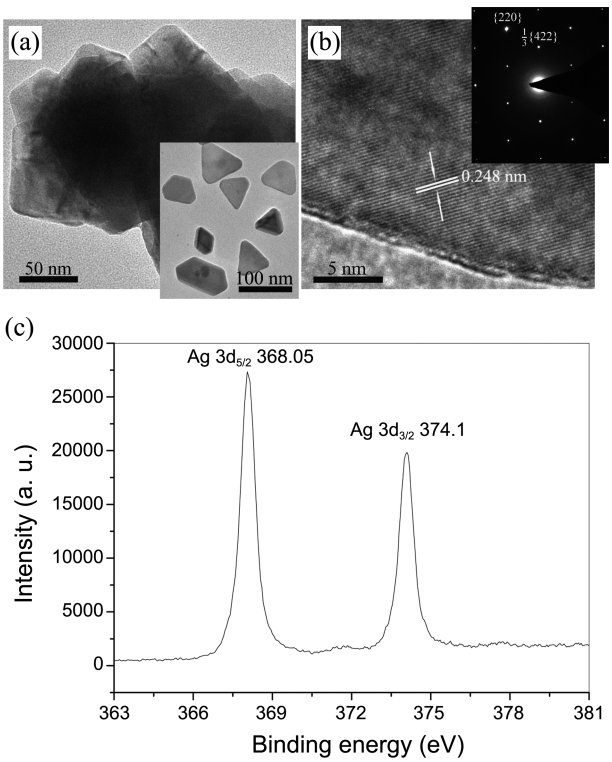

Figure 2. (a) TEM image of the silver nanoplates. The inset shows a picture of the dispersive nanoplates. (b) High-resolution TEM image taken from the nanoplate. The inset gives a typical SAED pattern taken from the nanoplates. (c) XPS spectrum of the as-prepared product.

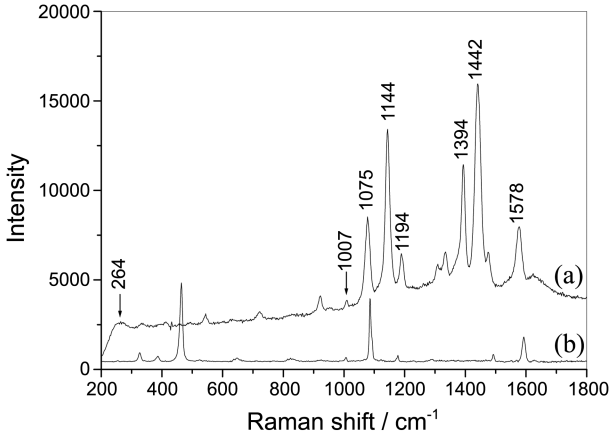

Figure 3. (a) SERS spectra of 4-ATP on the silver nanoplates. (b) The normal Raman spectra of solid 4-ATP. Laser power: 6.25 mW; integration time: 10 s.

appear at 368.05 eV and 374.1 eV, respectively, agreeing with that of Ag^0 (Figure 2(c)), which indicates that the nanoplates are composed of elemental silver.[19]

The formation of the Ag nanoplates is likely the outcome of the interplay between the faceting tendency of the stabilizer and growth kinetics.[20] Fn nanofibrils as stabilizing and structure-directing agent vary the surface energies of different crystal faces by preferentially interacting with specific planes of the particles, by which they can control the growth rates of various faces of Ag cores for tuning the shape of particles. Fn nanofibrils are chemically adsorbed onto the Ag nanoparticles surface through the formation of amide bonds.[17] It is documented that surface-free energy of Ag {111} facets is lower than that of {100} and {110}.[21] This suggests that the bonding ability and chemical reactivity of the {111} planes is relative weak. Thus, Fn nanofibrils preferentially adsorb onto the crystal facets other than {111} planes. This selectivity interaction between Fn nanofibrils and crystal lattice structure may not only influence the surface energies but also alter the distribution of surface concentration of this species. Fn nanofibrils are dynamically adsorbed and desorbed on the crystallographic planes. The resulting Ag atoms tend to assemble to the Ag nuclei to form the larger particles. The selective interaction enhances the growth rate along the specific facet direction, resulting in the formation of Ag nanoplates dominated by {111} facets.

SERS Activity of Silver Nanoplates. The silver nanoplates can serve as a substrate for SERS. 4-ATP was used as a target molecule to examine the SERS sensitivity of silver nanoplate aggregates. Simply, 20 μL of 1×10^{-7} M 4-ATP ethanol solution was dropped onto the sample surface, and then dried in air. Figure 3(a) shows the SERS spectrum of 4-ATP on the silver nanoplates. For comparison, the normal Raman spectrum of solid 4-ATP is given in Figure 3(b). The obvious difference between the two spectra is frequency shifts and some changes in the intensity for most of the bands. For example, the ν(CS) band shifts from 1085 cm^{-1} in Figure 3(b) to 1075 cm^{-1} in Figure 3(a), and ν(CC) band shifts from 1593 cm^{-1} to 1578 cm^{-1}. These changes in several main bands indicate that the thiol group of 4-ATP directly contacts with the surface of Ag nanoplate through forming a strong Ag-S bond.[15] Besides, the band at 464 cm^{-1} in curve b is missing in curve a, accompanied with the appearance of a new band at 264 cm^{-1} in curve a. This band belongs to the Ag-S stretching vibration.[15,22] The SERS spectra are dominated by the b_2 modes (in-plane, out-of-phase modes) at 1578, 1442, 1394, and 1144 cm^{-1}. They are assigned to the fundamental benzene ring vibrations (ν_{8a}, ν_{19b}, δ_{3b} and δ_{9b}, respectively). The predominance of the b_2 modes in the SERS spectrum implies that a greater extent of charge transfer (CT) from the nanoplates to 4-ATP occurs.[23] Furthermore, the enhancement of the a_1 modes (in-plane, in-phase modes) located at 1075 cm^{-1} can be clearly observed. The obvious enhancement of the a_1 modes indicates that the electromagnetic (EM) mechanism should also be considered.[15,23] The surface enhancement factor (EF) of 4-ATP on the substrate was calculated according to the following equation:

$$EF = (I_{SERS}/I_{Raman}) \times (M_{bulk}/M_{surface})$$

where I_{SERS} and I_{Raman} are the intensities in the SERS and normal Raman spectrum, respectively; M_{bulk} is the concentration of molecules in the bulk sample; and $M_{surface}$ is the concentration of adsorbed molecules. For the target molecule 4-ATP, in the sample area (1 μm in diameter) measured, $M_{surface}$ was calculated to be 1.2×10^4 μm^{-2}. Taking the laser spot (1 μm in diameter), the penetration depth (about 2 μm) and the density of 4-ATP (1.17 $g \cdot mL^{-1}$) into account,[24] The value of M_{bulk} was 0.82×10^{10} μm^{-2} in the detected solid sample area. For the vibrational modes at 1593 cm^{-1} (ν_{CC}), the EF was estimated to be about 1.2×10^7. Additionally, the intensity of the bands at 1442, 1394, and 1144 cm^{-1} in the SERS spectrum are tens of times that of the normal spectrum. This large enhancement implies that the SERS mechanism is complicated. We suggest that it is the result of the synergistic effect of CT and EM mechanism. In the present case, the interaction between the photon, adsorbed molecule and Ag nanostructure should be taken into account, namely that the formation of the SERS on the Ag nanoplate substrate ascribes to the combination of chemical and physical enhancement mechanism. The advantages of the nanoplate aggregates as SERS substrate are thirdfold. First, it has relatively large surface area for anchoring many probe molecules, resulting in great enhancement. Second, the close interaction of nanosheets can provide a broader surface plasmon resonance for optical scattering and enhance the electromagnetic field.[23] Third, the nanoscale roughness can furnish pathways for the hot electrons to the probe molecules.[25]

The silver nanoplates as substrate can be employed to detect biologically important 2-TU molecule. 2-TU and its derivatives show high antithyroid, antiviral, and antitumor activity.[26] Sensitive detection of 2-TU at low concentration is important for pharmokinetic and clinical studies. 20 μL of 1×10^{-4} M 2-TU ethanol solution was casting onto the sample surface, and then dried in air. Figure 4(a) presents the

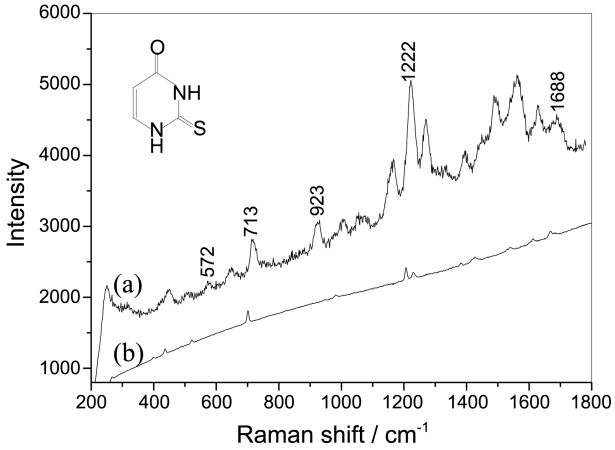

Figure 4. SERS spectra of 2-TU on the (a) presence and (b) absence of nanoplate aggregates.

SERS spectrum of 2-TU on the nanoplates. The spectrum is in good agreement with previous report.[27] Figure 4(b) gives the normal Raman spectrum of solid 2-TU. Relative to the normal Raman spectrum, the apparent difference in the SERS spectrum are the increase in the intensity for most of the bands. For example, the band located at 1222 cm^{-1} belonging to the in plane bending of C(5)-H and C(6)-H is obviously enhanced. The band observed at 923 cm^{-1} in the SERS spectrum corresponding to the in plane bending of N(3)CC and ring is very noticeable. However, it is not prominent in the normal Raman spectrum. The result indicates that the silver nanoplates as substrate may be a potential powerful tool for ultrosensitive detection of different analytes.

Conclusion

In summary, for the first time we report a novel way to synthesize silver nanoplates using Fn nanofibril as an architecture soft template. The synthesized nanoplates are highly efficient SERS substrate on the part to great detection sensitivity, good stability and reproducibility. This substrate can be used to detect low concentrated 4-ATP and 2-TU molecule. The silver nanoplates fabricated with the biological template could be an ideal system for the application in biosensors, pharmaceutical analysis and nanodevices design.

Acknowledgments. This work was financial supported by the Jilin Province Science and Technology Development Foundation of China under Grant No. 20120577, the Science and Technology Research Program of Education Bureau of Jilin Province (Grant No. 2011165) and the National Nature Science Foundation of China (Grant No. 21077041).

References

1. Kang, S. K.; Kim, Y.; Choi, I.; Lee, J.; Yi, J. *Microelectron Eng.* **2005**, *81*, 389.
2. Tan, Y.; Li, Y.; Zhu, D. *Langmuir* **2002**, *18*, 3392.
3. Chen, C.; Wang, L.; Jiang, G.; Yu, H. *Rev. Adv. Mater. Sci.* **2006**, *11*, 1.
4. Fullam, S.; Cottell, D.; Rensmo, H.; Fitzmaurice, D. *Adv. Mater.* **2000**, *12*, 1430.
5. Wei, G.; Reichert, J.; Jandt, K. D. *Chem. Commun.* **2008**, 3903.
6. Sau, T. K.; Murphy, C. J. *J. Am. Chem. Soc.* **2004**, *126*, 8648.
7. Kim, F.; Song, J. H.; Yang, P. *J. Am. Chem. Soc.* **2002**, *124*, 14316.
8. Jin, R.; Cao, Y.; Mirkin, C. A.; Kelly, K. L.; Schatz, G. C. Zheng, J. G. *Science* **2001**, *294*, 1901.
9. Tomczak, M. M.; Slocik, J. M.; Stone, M. O.; Naik, R. R. *Biochem. Soc. Trans.* **2007**, *35*, 512.
10. Tang, Z.; Wang, Y.; Podsiadlo, P.; Kotov, N. A. *Adv. Mater.* **2006**, *18*, 3203.
11. Sotiropoulou, S.; Sierra-Sastre, Y.; Mark, S. S.; Batt, C. A. *Chem. Mater.* **2008**, *20*, 821.
12. Ferguson, N.; Becker, J.; Tidow, H.; Tremmel, S.; Sharpe, T. D.; Krause, G.; Flinders, J.; Petrovich, M.; Berriman, J.; Oschkinat, H.; Fersht, A. R. *Proc. Natl. Acad. Sci. U.S.A.* **2006**, *103*, 16248.
13. Scheibel, T. *Curr. Opin. In Biotech.* **2005**, *16*, 427.
14. Wang, T.; Hu, X.; Dong, S. *J. Phys. Chem. B* **2006**, *110*, 16930.
15. Arnaudov, L. N.; de Vries, R. *Biomacromolecules* **2006**, *7*, 3490.
16. Wei, G.; Keller, T. F.; Zhang, J. T.; Jandt, K. D. *Soft Matter* **2011**, *7*, 2011.
17. Sun, Y.; Mayers, B.; Xia, Y. *Nano. Lett.* **2003**, *3*, 675.
18. Zheng, Y.; Zheng, L.; Zhan, Y.; Lin, X.; Zheng, Q.; Wei, K. *Inorg. Chem.* **2007**, *46*, 6980.
19. Sau, T. K.; Murphy, C. J. *J. Am. Chem. Soc.* **2004**, *126*, 8648.
20. Hu, J.; Chen, Q.; Xie, Z.; Han, G.; Wang, R.; Ren, B.; Zhang, Y.; Yang, Z.; Tian, Z. *Adv. Funct. Mater.* **2004**, *14*, 183.
21. Wei, G.; Wang, L.; Liu, Z.; Song, Y.; Sun, L.; Yang, Y.; Li, Z. *J. Phys. Chem. B* **2005**, *109*, 23941.
22. Sun, Y.; Wei, G.; Song, Y.; Wang, L.; Sun, L.; Guo, C.; Yang, T.; Li, Z. *Nanotechnology* **2008**, *19*, 115604 (8pp).
23. Sun, L.; Zhao, D.; Zhang, Z.; Li, B.; Shen, D. *J. Mater. Chem.* **2011**, *21*, 9674.
24. Wang, L.; Sun, Y.; Che, G.; Li, Z. *Appl. Surf. Sci.* **2011**, *257*, 7150.
25. Lindsay, R. H.; Romine, C. J.; Wong, M. Y. *Arch. Biochem. Biophys.* **1968**, *126*, 812.
26. Jena, B. K.; Raj, C. R. *Chem. Mater.* **2008**, *20*, 3546.